

## Improving the Yield and Quality of Tar during Co-pyrolysis of Coal and Cotton Stalk

Chuyang Tang,<sup>a, b</sup> Dexiang Zhang,<sup>a, \*</sup> and Xilan Lu<sup>a</sup>

Co-pyrolysis of Shenmu coal (SM) and cotton stalk (CS) at different blend ratios were carried out in a tubular furnace. The pyrolysis temperature was up to 600 °C at 5 °C/min and kept for 15 min. The results indicated that there was an interactive effect between SM and CS, which increased the tar yield. Moreover, the content of light components in co-pyrolysis tar from all CS/SM blend ratios was higher than that in the tar derived from SM pyrolysis. This interaction not only increased tar yields but also upgraded the quality of tar in the co-pyrolysis process. Compared with the co-pyrolysis of de-ashed CS and SM, the inherent minerals of CS had great effects on the co-pyrolysis tar yield. The analysis results of n-hexane soluble extracted from co-pyrolysis tar by gas chromatography/mass spectrometry indicated that the organic matters of CS had a significant effect on the alkene formation of tar during co-pyrolysis. The maximal tar yield was 13.73 wt% (daf) and the yield of n-hexane soluble reached 11.13 wt% (daf) under optimum conditions.

*Keywords:* Tar; Cotton stalk; Coal; Co-pyrolysis; Alkanes formation

*Contact information:* a: School of Resource and Environmental Engineering, East China University of Science and Technology, Key Laboratory of Coal Gasification and Energy Chemical Engineering of Ministry of Education, 130#, Meilong Road, Shanghai 200237, PR China; b: School of Architecture and Construction, University of Science and Technology Liaoning, 185#, Qianshan Road, Liaoning Province 114051, PR China; \*Corresponding author: zdx@ecust.edu.cn

### INTRODUCTION

As cotton-producing areas, the central and western regions of China have a large supply of biomass resources. The coal resources of the region are abundant; at present, coal is the main feedstock used for power generation in China. Cotton stalk agricultural residues are traditionally burned to directly generate energy. The direct combustion of coal and cotton stalk is inefficient and causes many health problems for human beings and significant damage to other creatures (Kolari *et al.* 2012). Thus, the co-utilization of coal and local biomass resources is beneficial to lower fossil fuel costs, CO<sub>2</sub> emissions, and transportation costs. Co-pyrolysis is a feasible methods to produce liquid fuels and high added-value chemicals.

Biomass and coal have different structures and constituents. These differences in properties lead to individual reactivity and thermal characteristics during co-pyrolysis. The pyrolysis of coal starts with thermal cleavage of covalent bonds to generate volatile radical fragments (He *et al.* 2014). Biomass has a much higher pyrolysis rate and its pyrolysis mostly occur within a narrow temperature range of 200 to 375 °C (Vassilev *et al.* 2010; Cheng *et al.* 2014). Due to the high hydrogen and carbon molar ratio, biomass may provide free radicals to stabilize the large radical fragments that result from the cleavage of coal during co-pyrolysis (Soncini *et al.* 2013).

Some studies have investigated the transfer of biomass volatiles to the coal structure resulting in improving the decomposition of coal (Sonobe *et al.* 2008; Krerkkaiwan *et al.* 2013). Li *et al.* (2013) reported that biomass promoted secondary reactions of co-pyrolysis. Yang *et al.* (2014) found that the addition of biomass decreased the tar yield and influenced tar composition during co-pyrolysis. However, there still has been controversy about the synergy effect (Weiland *et al.* 2012; Kirtania and Bhattacharya 2013). Besides, some studies showed that minerals had positive effects in the thermal decomposition of biomass and coal. Wei *et al.* (2011) indicated that biomass with high holocellulose and ash content produced more hydrogen during pyrolysis. Alkali composition was also associated with a decrease the initial reaction temperature and an improvement in the thermal decomposition of biomass (Shimada *et al.* 2008). Some studies documented that alkali metals such as  $K_2CO_3$ ,  $CaO$ , and  $Al_2O_3$  showed positive effects on the reactivity and kinetic characteristics of coal pyrolysis (Liu *et al.* 2004; Abbasi-Atibeh and Yozgatligil 2014). Mourant *et al.* (2011) indicated that the removal of alkaline earth metallic species decreased the light organic compounds of bio-oil on biomass pyrolysis. Most of the previous studies focused on the causes of synergy effects. These works provide lots of worthy references for the research of co-pyrolysis. Nevertheless, the literature about the effect factors of tar yield and quality are still rare.

In the present work, pyrolysis tests of Shenmu coal (SM), cotton stalk (CS), and their blend were carried out in a tubular furnace. Tar quality was determined by the content of n-hexane soluble in the tar. The co-pyrolysis of de-ashed cotton stalk (DACS)/SM and  $K_2CO_3$ /SM were used to investigate the different effects of organic matters and minerals in CS on the tar yields. The components of n-hexane soluble were further measured and compared the quality of tar derived from SM, CS/SM, and DACS/SM.

## EXPERIMENTAL

### Materials

The Shenmu coal (SM) sample was low grade, low ash, and high volatile bituminous coal from Shanxi province China. Cotton stalk (CS) was obtained from local farms. The air-dried samples were milled and sieved to obtain fractions of particle size less than 180  $\mu m$  in diameter for both SM and CS. The samples were dried at 105 °C for 2 h and then stored in a desiccator. CS/SM blends were prepared by physical mixing at biomass and coal weight ratios of 5/100, 10/100, 15/100, 20/100, 25/100, 30/100, and 50/100, respectively. Ultimate analysis was determined by a Macro Cube (Elementar, Germany). The properties of SM and CS were presented in Table 1. The relative error obtained by reproducing three times the same experiment, equal  $\pm 2\%$ .

### Methods

#### *De-ashing treatment*

Briefly, the de-ashing treatments of CS consist of acid washing. The samples of CS were occasionally stirred and soaked with 15 wt% HCl solution and 15 wt% HF solution at 70 °C for 24 h in sequence. Then, the resulting solid was filtered and washed with distilled water until the filtrate was neutral (Das *et al.* 2004). Finally, the solid matter was air dried and then stored in a desiccator. Ashing temperature of the de-ashing CS (DACS) was set at 575 °C according to ASTM E1755. The ash percentage of DACS was reduced to as low as 0.39 wt%. Table 1 lists the proximate and ultimate analyses of DACS.

**Table 1.** Proximate and Ultimate Analyses of the Samples

Sample	SM	CS	DACS
Proximate analysis (wt.%)			
Moisture (ad <sup>a</sup> )	3.78	2.31	4.97
Ash (d <sup>a</sup> )	8.63	4.13	0.39
Volatile Matter (daf <sup>a</sup> )	37.97	78.88	38.37
Fixed Carbon (daf)	62.03	21.12	61.63
Ultimate analysis (wt%, daf)			
Carbon, C	84.24	48.11	60.82
Hydrogen, H	5.49	6.02	4.23
Nitrogen, N	1.08	0.98	0.43
Sulfur, S	0.32	0.19	0.19
Oxygen, O (diff <sup>b</sup> )	8.88	44.70	34.34
<sup>a</sup> ad= air dried basis, d= dry basis, daf= dry and ash free basis			
<sup>b</sup> Calculated by difference			

### Apparatus and methods

The co-pyrolysis was performed in a tubular furnace (Nasren GDL-B-II, China), and its schematic diagram is shown in Fig. 1. The tubular furnace was made of cast copper. Five 1 kW electric heaters were installed inside the furnace to heat the quartz tubular reactor to the desired temperature. The thermocouple was close to the reactor in order to measure the heating temperature accurately. For every experimental run, about 10 g of the sample was fed into the tubular reactor. Thereafter the reactor was pushed into the furnace and heated to 600 °C at a rate of 5 °C/min and then kept for 15 min. The condenser was immersed in an ice-water bath to keep the expected cooling conditions near 0 °C. The volatiles released from the sample were cooled in a condenser in series to collect the condensable components.

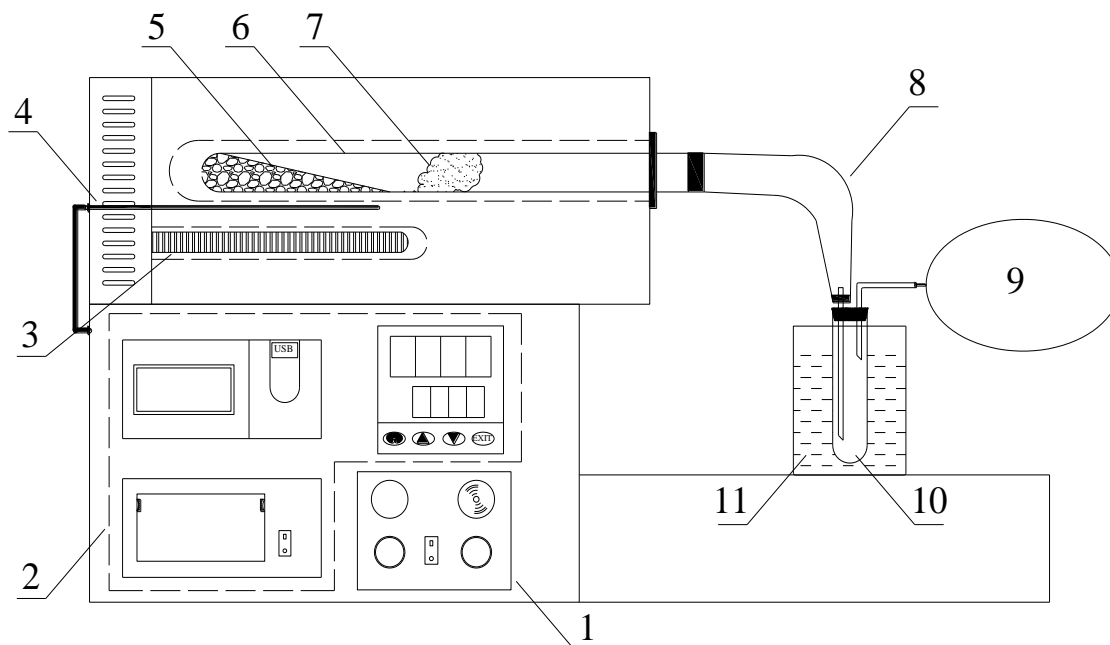


**Fig. 1.** Schematic diagram of the pyrolysis apparatus. 1. Heating control; 2. Temperature regulation; 3. Bolt electric heaters; 4. Thermocouple; 5. Samples; 6. Tubular reactor; 7. Asbestos wool; 8. Plain bend; 9. Gas bag; 10. Condenser; 11. Ice bath

The liquid products in the reactor, condenser, and pipeline were recovered by washing with acetone (AR grade) as a solvent into a round-bottom flask. The liquid (tar and water) yield of pyrolysis was determined by the mass difference of the condenser, reactor, and pipeline before and after washing. The char yield was determined by weighing the amount of the solid residues in the reactor after the liquid product was washed. A rotary evaporator was used to remove the acetone from the obtained washing liquid. The appropriate amount of n-hexane was then added into the round bottom flask to extract light components (n-hexane soluble) from the residue consisting of tar and water according to a standard method (ASTM D91-02 2012). Finally, the water was separated from n-hexane insoluble by reduced pressure evaporation. Meanwhile, a parallel experiment of co-pyrolysis was carried out and the water was washed subsequently by toluene (AR grade) from the condenser, reactor, and pipeline.

The total water yield was measured by toluene entrainment method (ASTM D4006-11 2012). The pyrolytic water yield was determined by the total water yield and proximate analyses of SM and CS. The tar yield was the difference value of the liquid yield and the water yield. The n-hexane soluble yield was equal to the tar yield minus the n-hexane insoluble yield in tar. The statistical analyses of the data obtained by co-pyrolysis showed that the maximum relative error of tar yield and char yield were  $\pm 2.4\%$  and  $\pm 2.2\%$ , respectively.

#### *Analytical instruments and procedure*

A thermogravimetric analyser of TG-DTA/DSC (Setaram, France) was used to investigate the pyrolysis characteristics of SM and CS. During the heating process, the samples were heated up to 1000 °C at 5 °C/min. High-purity nitrogen was used as the purge gas and the flow rate was kept constant at 60 mL/min. The results are shown in Fig. 2. The mineral composition of CS ash was analyzed by X-Ray Fluorescence (Shimadzu XRF-1800, Japan). The CS ash was obtained from the CS ashing according to ASTM E1755. The XRF results of CS ash are listed in Table 2. The compounds in the n-hexane soluble extracted from the pyrolysis tar were characterized by GC-MS (Agilent 5975C, USA). High-purity helium was chosen as the carrier gas. The content of each compound in the n-hexane soluble was calculated as the relative peak area against the total peak area, excluding that of solvent, in the total ion chromatogram of GC-MS. The yield of each compound was defined as the mass percentages of the product against the mass of the dry and ash free test sample.

**Table 2.** XRF Results of CS Ash (Wt.%)

Sample	K <sub>2</sub> O	CaO	MgO	SiO <sub>2</sub>	P <sub>2</sub> O <sub>5</sub>	Na <sub>2</sub> O	Al <sub>2</sub> O <sub>3</sub>	Fe <sub>2</sub> O <sub>3</sub>
Ash of CS	28.36	21.04	10.63	10.20	8.64	4.86	2.36	1.81

## RESULTS AND DISCUSSION

### TG Analyses of SM and CS

The TGA and DTG curves of SM and CS are shown in Fig. 2. The initial thermal decomposition ( $T_1$ ) of SM was at about 380 °C, and the maximal pyrolysis rate was found to be 0.0567 mg/min at 437 °C. A major loss of weight, *i.e.*, the main devolatilization, occurred between 380 °C and 510 °C. The devolatilization of SM was essentially

completed by about 550 °C. The  $T_1$  of CS started at approximately 260 °C. The maximal pyrolysis rate of CS (0.2162 mg/min) occurred at 310 °C. The weight loss of CS was mainly seen within the temperature range of 260 to 340 °C. After 450 °C, the weight loss rate of CS eventually became constant. It was observed that the maximal pyrolysis rate of CS was higher than that of SM. Compared with SM, the decomposition of CS mainly occurred in a range of 200 to 400 °C because the cellulose and lignin of CS, which are linked together with relatively weak ether bonds, will be broken at lower temperatures (Zhang *et al.* 2012, 2013).

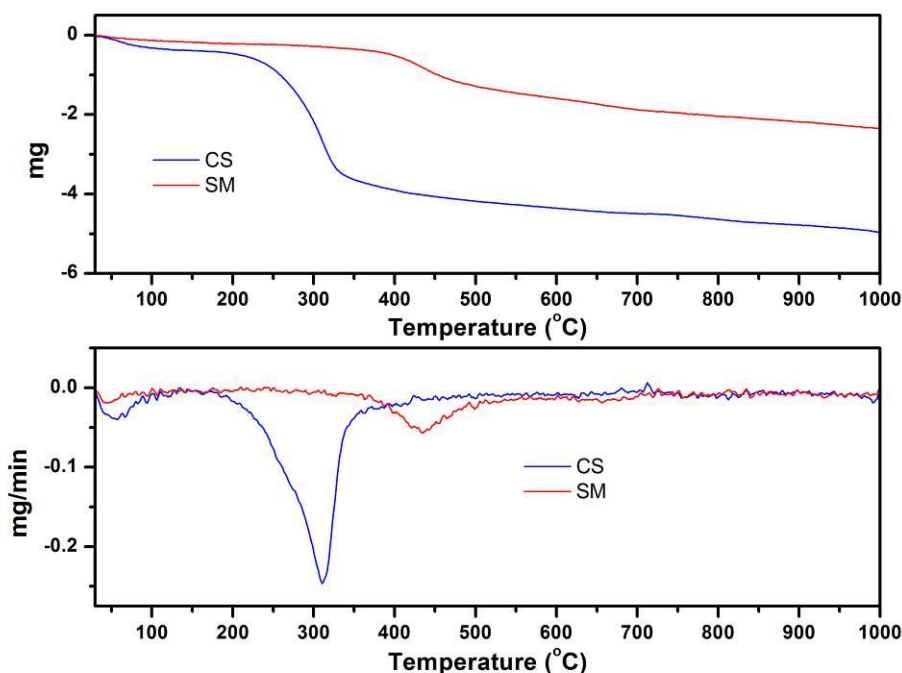


Fig. 2. TGA and DTG curves of SM and CS (heating rate 5 °C/min)

### Pyrolytic Characteristics of SM, CS, and DACS

The distribution of pyrolysis products for SM, CS, and DACS in the tubular furnace are listed in Table 3. CS pyrolysis had the maximal tar yield, water yield, and n-hexane soluble yield of 19.46 wt% (daf), 26.84 wt% (daf), and 10.74 wt% (daf), respectively. CS pyrolysis produced more tar and n-hexane soluble than SM pyrolysis. The water yield of SM pyrolysis was 6.10 wt% (daf). The water yield of CS pyrolysis was much higher than that of SM pyrolysis due to the higher oxygen content of CS. The char yield of CS pyrolysis was lower than that of SM pyrolysis corresponding to the proximate results of CS and SM.

Table 3. Product Distribution for Pyrolysis of SM, CS and DACS (Wt.%, Daf)

Samples	Tar	Water	Char	n-hexane soluble
SM	11.78	6.10	73.92	8.18
CS	19.46	26.84	29.21	10.74
DACS	9.59	11.66	53.63	8.74

As shown in Table 3, the tar and n-hexane soluble yield of DACS pyrolysis were 9.59 wt% (daf) and 8.74 wt% (daf), which were obviously lower than those of CS pyrolysis because of the de-ashed treatment. The water yield of DACS pyrolysis was 11.66 wt% (daf), lower than that of SM pyrolysis. Compared with the CS pyrolysis products, DACS pyrolysis produced less water and more char. The results showed that the inherent minerals in CS evidently promoted CS decomposition to increase the yields of tar and n-hexane soluble during CS pyrolysis.

### Co-pyrolytic Characteristics

To determine the interactive effects that occurred in co-pyrolysis of CS and SM, the experimental values were compared with calculated ones from the additive model. The additive model assumed that there were no interactions between the two samples during co-processing so that the calculated values were sum of the values of individual samples proportional to their blending weight ratio as (Eq. 1),

$$X_{cal} = r_1X_1 + r_2X_2 \quad (1)$$

where  $X_{cal}$  was the calculated value from the additive model,  $X_i$  was the measured experimental value of sample  $i$  separately, and  $r_i$  was the blending ratio of sample  $i$ .

### Co-pyrolysis of CS/SM

The product yields from the co-pyrolysis of CS/SM are shown in Fig. 3. All yields are represented in mass percent on a dry and ash free basis. The results indicated that there is an obviously interactive effect between CS and SM that increased the yields of tar and n-hexane during co-pyrolysis. The interactive effect has not been published.

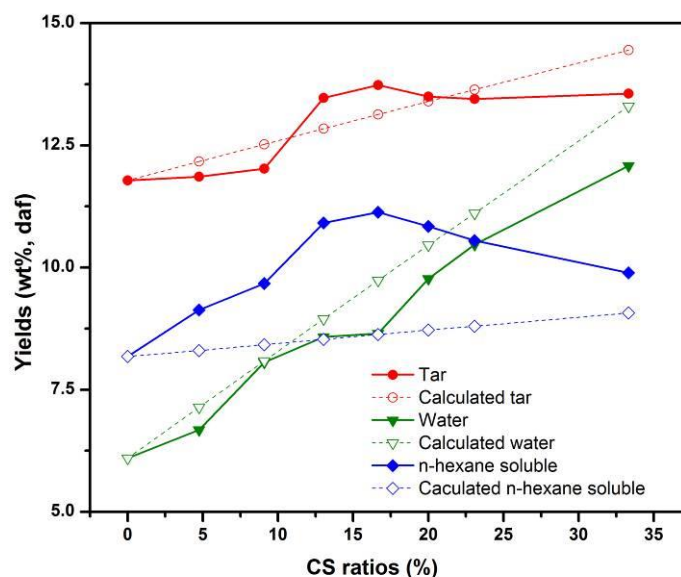


**Fig. 3.** Difference of product yields with the calculated values in co-pyrolysis of CS and SM

With the increase of CS content in blends, the tar yields first increased and then decreased. When the CS ratios in the blend of CS and SM were less than 10% or more than 25%, the tar yields were less than the calculated values and the tar yields were more than the calculated values, within the ratio range of CS addition from 10% to 25% in the blend

of CS and SM. The maximal tar yield occurred at the CS/SM ratio of 20/100 and was higher than its calculated value. The results showed that the proper ratio of CS could improve the co-pyrolysis of CS and SM to produce more tar than SM pyrolysis alone.

The content of n-hexane soluble was known to represent the quality of tar (Li *et al.* 2015). The interactive effects of CS and SM improved the content of light components (n-hexane soluble) in co-pyrolysis tar. Based on the blend ratio of co-pyrolytic experimental, the n-hexane yields were always higher than the relevant calculated values. With the increasing of the CS ratio in blends, the n-hexane soluble yields first increased and then decreased, similar to the variation of tar yield, the maximal value was also obtained at the ratio of 20/100 (CS/SM) and 28.97% higher than its calculated value (8.63 wt%, daf). Moreover, the maximal n-hexane soluble yield of CS/SM co-pyrolysis was higher than that of SM pyrolysis and CS pyrolysis. With the increase of CS content in blends, the water yields were always increased and lower than its calculated values.

As is shown in Fig. 3 and Table 3, the CS addition promoted the co-pyrolysis of CS/SM to produce more tar and n-hexane soluble than SM pyrolysis. The maximal tar yield of co-pyrolysis was 13.73 wt% (daf) and 16.55% higher than the tar yield of SM pyrolysis (11.78 wt%, daf). The maximal yield of n-hexane soluble (11.73 wt%, daf) was 43.40% higher than that of SM pyrolysis (8.18 wt%, daf). Therefore, CS can not only increase tar yields but also upgrade the quality of tar on co-pyrolysis.

The variation of tar yields could be accounted for based on a radical mechanism (He *et al.* 2014). Compared with SM pyrolysis, more light components were formed and more tar was produced during co-pyrolysis because the macromolecular free radicals released from CS could stabilize macromolecule free radicals generated from SM pyrolysis (Sonobe *et al.* 2008). The free radicals derived from CS might increase the yield of tar and accelerate the formation of light components. Because the thermal weight loss of CS and SM mainly occurred in a different temperature range, CS and SM barely had an interactive effect on the generation of free radicals, although the increasing of free radicals should be proportional to the CS addition. There should be an optimal blending ratio of CS and SM corresponding to the maximal yield of tar and n-hexane soluble as shown in Fig. 3. Because the generation of free radicals was affected by the compositions and structure of CS and SM, further experiments were performed to explore the mechanism.

### Effects of Inherent Minerals in Biomass during Co-pyrolysis

In order to reveal the inherent mineral effect of CS on product distribution during co-pyrolysis of CS/SM, the co-pyrolysis of DACS/SM was carried out for comparison. Wang *et al.* (2014) found that the inherent minerals could enhance thermal decomposing of biomass. Compared with the results of CS pyrolysis and DACS pyrolysis in Table 3, the yields of tar and n-hexane soluble of DACS pyrolysis decreased. CS addition had far more improvement on tar yield than the DACS addition did, as shown in Fig. 4a, especially when the blend ratios were higher than 20/100. It was seen that the inherent minerals in CS obviously catalyzed the co-pyrolysis of CS/SM to improve the formation of tar.

The water yields of CS/SM were also higher than that of DACS/SM when the blend ratios were higher than 5/100 in Fig. 4c. It was noted that both the co-pyrolysis of CS/SM and DACS/SM could produce more n-hexane soluble than SM pyrolysis alone in Fig. 4b. The results showed that the organic matter of CS could increase the content of light components in the co-pyrolytic tar. When the ratio of the blend was less than 10/100, the n-hexane soluble yields of CS/SM were close to that of DACS/SM. The tar quality of CS/SM was obviously better than that of DACS/SM when the ratios exceeded 20/100.

Compared with the variation of char yields in Fig. 4d, the pyrolytic rate of CS/SM was higher than that of DACS/SM. Based on the results, the inherent mineral in CS improved the thermal decomposition of the blend of CS and SM during co-pyrolysis. When the additive ratio of the blend was lower than 10/100, the n-hexane soluble yield of CS/SM co-pyrolysis was less than that of DACS/SM co-pyrolysis. When the additive ratio was higher than 10/100, the CS addition obviously increased the yield and upgraded the quality of tar.

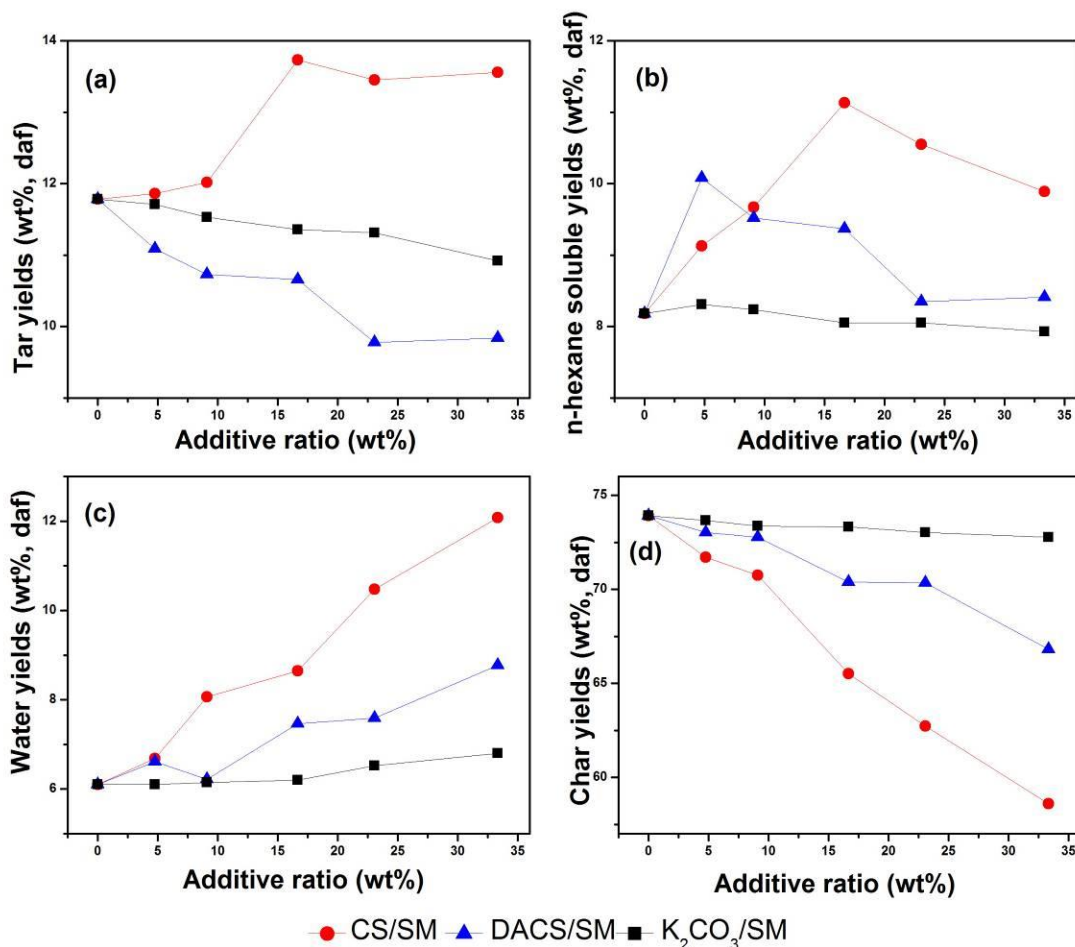


**Fig. 4.** Production distribution from co-pyrolysis of CS/SM, DACS/SM and K<sub>2</sub>CO<sub>3</sub>/SM (a: tar yields, b: n-hexane soluble yields, c: water yields, d: char yields)

### Effects of Additional Minerals on SM Pyrolysis

The addition of alkali is well known to catalyze coal pyrolysis. The minerals inherently present in CS might have an effect not only on CS, but also on SM during co-pyrolysis. As shown in Table 2, the main minerals of cotton stalk are potassium and calcium. The calcium of CS exists in the cytoderm and the potassium in ionic form dissolves in the plant juice which flows in vessel. Because the particle size both of SM and CS was less than 180  $\mu\text{m}$ , the sylvite in CS could touch directly with SM particles in the blending but calcium in the cytoderm could be released from CS particles during pyrolysis. Therefore, the pyrolysis of K<sub>2</sub>CO<sub>3</sub>/SM was performed to investigate the catalytic effects of K<sub>2</sub>CO<sub>3</sub> on SM pyrolysis. Volatilization of the inorganic components in biomass is known to be strongly dependent on the pyrolysis temperature (Keown *et al.* 2008; Liao *et al.* 2015). K<sub>2</sub>CO<sub>3</sub> was sieved to obtain fractions of particle size less than 180  $\mu\text{m}$ . Since a little of the

inorganic components were released with temperature lower than 600 °C during pyrolysis (Du *et al.* 2014), the blend ratios of K<sub>2</sub>CO<sub>3</sub>/SM were 0.034/100, 0.067/100, 0.135/100, 0.202/100, and 0.337/100, which was determined by the results of XRF (listed in Table 2) and matched with the blend ratios of CS in co-pyrolysis of CS/SM.

With the increasing of K<sub>2</sub>CO<sub>3</sub> addition, the tar yield of K<sub>2</sub>CO<sub>3</sub>/SM pyrolysis was decreased and the n-hexane soluble yield was also decreased but close to that of SM pyrolysis in comparison with SM pyrolysis. Figure 4a shows that the yields of tar derived from pyrolysis of K<sub>2</sub>CO<sub>3</sub>/SM were lower than the yields of CS/SM and higher than the yields of DACS/SM. As shown in Fig. 4b, the n-hexane soluble yields of K<sub>2</sub>CO<sub>3</sub>/SM pyrolysis were always lower than that of co-pyrolysis CS/SM and DACS/SM, and yet the variation of char yields was quite the contrary. Though K<sub>2</sub>CO<sub>3</sub> has been documented to catalyze the pyrolysis of coal (Patwardhan *et al.* 2010), the K<sub>2</sub>CO<sub>3</sub> addition had less effect on the decomposition of SM, possibly due to the low pyrolysis temperature and little additive amount as shown in Fig. 4d. With the results of Fig. 4a and Fig. 4c, K<sub>2</sub>CO<sub>3</sub> addition could increase the water and decrease the tar yield on SM pyrolysis.

In a word, the inherent minerals of CS could catalyze co-pyrolysis of CS/SM to improve the tar yield and quality. Moreover, the inherent minerals of CS had more influence on the product distribution than the additional minerals during the co-pyrolysis process. The catalytic effect of inherent minerals in CS could be due to its dispersibility and the occurrence form during co-pyrolysis of CS and SM.

### n-Hexane Soluble Characterization from Pyrolysis Tar

The light components were extracted from tar by n-hexane. The characteristics of tar quality could be understood by analyses of n-hexane soluble components. The n-hexane solubles obtained by the pyrolysis of SM, CS, CS/SM, and DACS/SM at 20/100 ratio were detected by GC-MS. Table 4 shows the main compounds identified in the n-hexane soluble fraction according to the peak intensities and areas. Significant interaction effects were found when comparing species of the n-hexane soluble components of co-pyrolysis tar and SM pyrolysis tar with those of CS pyrolysis tar. Those main components of the n-hexane soluble derived from the tar of CS pyrolysis, such as cyclopentane and methyl-, cyclohexane, were not detected in the n-hexane soluble fraction derived from co-pyrolysis of CS/SM and DACS/SM. It is known that cyclohexane and its derivatives are produced by the cellulose pyrolysis (Mohan *et al.* 2006). This showed that the free radicals generated from CS pyrolysis combined with those from SM pyrolysis during co-pyrolysis of CS/SM.

The compounds in n-hexane soluble were classified into nine groups, including alkanes, benzenes, phenols, indene, naphthalene, fluorene, anthracene, phenanthrene, biphenyl, and their related derivatives. The yields of the compounds are illustrated in Fig. 5. It was obvious that the dominant chemical was alkane. Comparatively, the addition of CS greatly increased the alkane yield of CS/SM which was 6.24 wt% (daf, coal) and was 70.49% higher than the yield of SM (3.66 wt%, daf, coal) and 7.22% higher than the yield of DACS/SM (5.82 wt%, daf, coal). While other component yields were close to those of SM and DACS/SM, the alkane yield of CS/SM was higher than that of DACS/SM, probably due to the inherent minerals of CS. Moreover, the alkane yield of DACS/SM was 59.02% higher than the yield of SM. The results demonstrate that the addition of CS and DACS also improved the alkane content in co-pyrolysis tar. The formation of alkanes was evident from the side chain cleavage during coal pyrolysis.

**Table 4.** Main Components of n-Hexane Soluble

Peak no. Compounds		Relative area (%)			
		SM	CS/SM <sup>a</sup>	DACS/SM <sup>a</sup>	CS
1	Nonane	1.66	1.16	0.76	—
2	Phenol, 3-methyl-	1.77	1.01	0.71	—
3	Phenol, 2-methyl-	2.75	1.93	1.39	0.70
4	Phenol, 2,4-dimethyl-	1.91	1.48	1.95	0.25
5	Phenol, 2-ethyl-	0.33	1.27	1.07	0.19
6	Dodecane	1.22	1.09	0.90	0.22
7	Naphthalene, 1-methyl-	0.98	0.91	0.82	—
8	Tetradecane	1.25	1.29	1.15	—
10	Pentadecane	1.57	1.73	1.50	—
11	Phenol, 2,4-bis(1,1-dimethylethyl)	0.86	1.02	1.71	—
12	1-Naphthalenol	0.26	1.11	0.31	—
13	3,5-Dimethyl-4-(2-furyl)pyridine	—	—	1.91	—
14	Naphthalene, 1,2,3,4-tetrahydro-5, 6,7,8-tetramethyl-	0.94	—	—	—
15	Hexadecane	1.29	1.68	1.70	—
16	Dibenzofuran, 4-methyl-	1.03	0.83	0.46	—
17	Heptadecane	1.18	1.41	1.43	—
20	Octadecane	1.18	1.27	1.24	—
21	Nonadecane	1.44	—	—	—
22	Hentriacontane	0.51	0.28	1.18	—
23	Eicosane	2.35	2.82	2.94	0.15
24	Heneicosane	2.22	2.83	2.96	0.19
25	Naphthalene, 7-butyl-1-hexyl-	0.99	1.15	1.11	—
26	Docosane	—	2.06	1.97	—
27	Phenanthrene, 1-methyl-7-(1-methyl ethyl)-	2.86	2.87	2.17	—
28	Nonadecane	1.82	—	—	—
29	Tricosane	—	1.90	1.87	—
30	9-Octadecenamide, (Z)-	2.01	1.99	1.91	—
31	Tetracosane	1.61	1.66	1.67	—
32	Pentacosane	1.49	1.75	1.44	0.26
33	Silicic acid, diethyl bis(trimethylsilyl) ester	1.51	0.50	0.48	—
34	Pentane, 2,2-dimethyl-	—	—	—	1.36
35	Cyclopentane, methyl-	—	—	—	45.63
36	Cyclohexane	—	—	—	26.76
37	Propanoic acid, 2-methyl-, anhydri	—	—	—	1.68
38	Phenol, 2-methoxy-	—	—	—	1.42

<sup>a</sup> blend ratio is 20/100  
— not detected

Because the alkanes in the n-hexane soluble fraction derived from tar were mostly chain-hydrocarbon, and the main light components of bio-oil such as cyclopentane, methyl, and cyclohexane were not detected, the side chain cleavage from SM could combine with the free radicals derived from CS pyrolysis to form more alkanes than SM pyrolysis during the co-pyrolysis. Therefore, the formation of alkanes was influenced remarkably by the free radicals from decomposition of organic matter in CS.

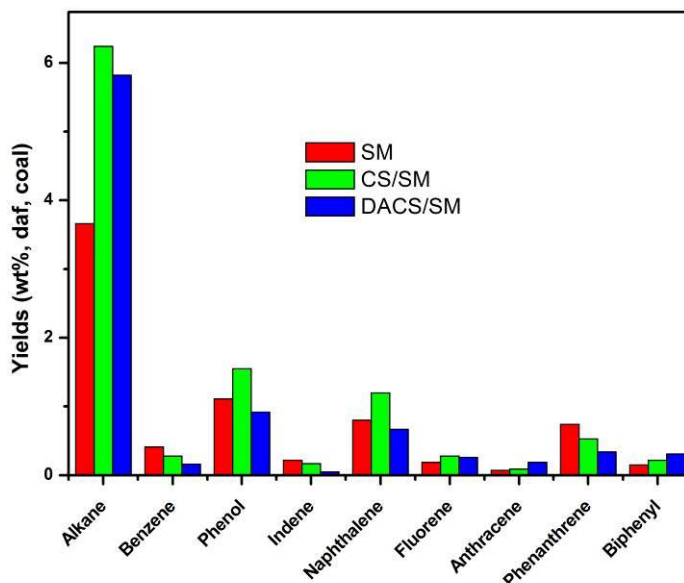


**Fig. 5.** Yields of major chemicals in n-hexane soluble for pyrolysis of SM, CS/SM, and DACS/SM at the ratio of 20/100

## CONCLUSIONS

1. Co-pyrolysis of CS and SM was performed in a tubular furnace. An interactive effect promoted the yields of tar and the light component in pyrolytic tar during the co-pyrolysis. The yields of pyrolysis water and char from co-pyrolysis were less than the calculated values. The tar yields were higher than the calculated values within the range of CS ratio from 10% to 25% and the n-hexane soluble yields were always higher than relevant calculated values in the range of experimental proportion.
2. The results of DACS/SM co-pyrolysis indicated that the organic matter of CS increased the content of light components in the co-pyrolytic tar. Compared with the co-pyrolysis of DACS/SM, the inherent minerals of CS had catalytic effects on the co-pyrolysis of CS/SM and increased the yields of tar and n-hexane soluble in the co-pyrolysis of CS/SM. The comparative test results of  $K_2CO_3$  and SM showed that the additional minerals had relatively less catalytic effects than the inherent minerals of CS during co-pyrolysis. The significant catalytic effects of inherent minerals in CS could have been due to its dispersibility and the form of occurrence in biomass. The maximal tar yield of CS/SM co-pyrolysis was 13.73 wt% (daf) and about 2 points higher than that of SM pyrolysis (11.78wt%, daf). The n-hexane soluble yield of CS/SM co-pyrolysis was 11.13 wt% (daf) and higher than the both of SM pyrolysis and CS pyrolysis alone.

3. The alkane yield of CS/SM co-pyrolysis tar was obviously higher than that of SM pyrolysis. The maximal yield of alkanes in the tar was 6.24 wt% (daf) in co-pyrolysis of CS/SM and 70.49% higher than that of SM pyrolysis alone. The results indicated that the CS addition can accelerate the formation of alkanes in tar during CS/SM co-pyrolysis.

## ACKNOWLEDGEMENTS

This work was supported by the National Basic Research Program of China (973 program, 2011CB201304).

## REFERENCES CITED

- Abbasi-Atibeh, E., and Yozgatligil, A. (2014). "A study on the effects of catalysts on pyrolysis and combustion characteristics of Turkish lignite in oxy-fuel conditions," *Fuel* 115, 841-849. DOI: 10.1016/j.fuel.2013.01.073
- ASTM D 4006-11. (2012). "Standard test method for water in crude oil by distillation," *Annual Book of Standards*, section 5, Textiles, ASTM, West Conshohocken, PA.
- ASTM D 91-02. (2012). "Standard test method for precipitation number of lubricating oils," *Annual Book of Standards*, section 5, Textiles, ASTM, West Conshohocken, PA.
- Cheng, H., Wu, S., and Liu, C. (2014). "Study on the mechanism of the pyrolysis of a lignin monomeric model compound by in situ FTIR," *BioResources* 9(3), 4441-4448. DOI: 10.15376/biores.9.3.4441-4448
- Das, P., Ganesh, A., and Wangikar, P. (2004). "Influence of pretreatment for deashing of sugarcane bagasse on pyrolysis products," *Biomass. Bioenergy*. 27(5), 445-457. DOI: 10.1016/j.biombioe.2004.04.002
- Du, S., Yang, H., Qian, K., Wang, X., and Chen, H. (2014). "Fusion and transformation properties of the inorganic components in biomass ash," *Fuel* 117(30), 1281-1287. DOI: 10.1016/j.fuel.2013.07.085
- He, W., Liu, Q., Shi, L., Liu, Z., Ci, D., Lievens, C., and Guo, X. (2014). "Understanding the stability of pyrolysis tars from biomass in a view point of free radicals," *Bioresour. Technol.* 156, 372-375. DOI: 10.1016/j.biortech.2014.01.063
- He, W., Liu, Z., Liu, Q., Ci, D., Lievens, C., and Guo, X. (2014). "Behaviors of radical fragments in tar generated from pyrolysis of 4 coals," *Fuel* 134(15), 375-380. DOI: 10.1016/j.fuel.2014.05.064
- Keown, D., Hayashi, J., and Li, C. (2008). "Effects of volatile-char interactions on the volatilization of alkali and alkaline earth metallic species during the pyrolysis of biomass," *Fuel* 87(7), 1187-1194. DOI: 10.1016/j.fuel.2007.05.056
- Kirtania, K., and Bhattacharya, S. (2013). "Pyrolysis kinetics and reactivity of algae-coal blends," *Biomass. Bioenergy* 55, 291-298. DOI: 10.1016/j.biombioe.2013.02.019
- Kolari, P., Bäck, J., Taipale, R., Ruuskanen, T.M., Kajos, M.K., Rinne, J., Kulmala, M., and Hari, P. (2012). "Evaluation of accuracy in measurements of VOC emissions with dynamic chamber system," *Atmos. Environ* 62, 344-351. DOI: 10.1016/j.atmosenv.2012.08.054

- Krerkkaiwan, S., Fushimi, C., Tsutsumi, A., and Kuchonthara, P. (2013). "Synergetic effect during co-pyrolysis/gasification of biomass and sub-bituminous coal," *Fuel Process. Technol.* 115, 11-18. DOI: 10.1016/j.fuproc.2013.03.044
- Li, S., Chen, X., Wang, L., Liu, A., and Yu, G. (2013). "Co-pyrolysis behaviors of saw dust and Shenfu coal in drop tube furnace and fixed bed reactor," *Bioresour. Technol.* 148, 24-29. DOI: 10.1016/j.biortech.2013.08.126
- Li, X., Xue, Y., Feng, J., Yi, Q., Li, W., Guo, X., and Liu, K. (2015). "Co-pyrolysis of lignite and Shendong coal direct liquefaction residue," *Fuel* 144(15), 342-348. DOI: 10.1016/j.fuel.2014.12.049
- Liao, Y., Cao, Y., Chen, T., and Ma, X. (2015). "Experiment and simulation study on alkalis transfer characteristic during direct combustion utilization of bagasse," *Bioresour. Technol.* 194, 196-204. DOI: 10.1016/j.biortech.2015.06.121
- Liu, Q., Hu, H., Zhou, Q., Zhu, S., and Chen, G. (2004). "Effect of inorganic matter on reactivity and kinetics of coal pyrolysis," *Fuel* 83(6), 713-718. DOI: 10.1016/j.fuel.2003.08.017
- Mohan, D., Pittman, C.U., and Steele, P. H. (2006). "Pyrolysis of wood/biomass for bio-oil: a critical review," *Energy. Fuels.* 20(3), 848-889. DOI: 10.1021/ef0502397
- Mourant, D., Wang, Z., He, M., Wang, X.S., Garcia-Perez, M., Ling, K., and Li, C. (2011). "Mallee wood fast pyrolysis: Effects of alkali and alkaline earth metallic species on the yield and composition of bio-oil," *Fuel* 90(9), 2915-2922. DOI: 10.1016/j.fuel.2011.04.033
- Vassilev, S. V., Baxter, D., Andersen, L. K., and Vassileva, C. G. (2010). "An overview of the chemical composition of biomass," *Fuel* 89(5), 913-933. DOI: 10.1016/j.fuel.2009.10.022
- Patwardhan, P. R., Satrio, J. A., Brown, R. C., and Shanks, B. H. (2010). "Influence of inorganic salts on the primary pyrolysis products of cellulose," *Bioresour. Technol.* 101(12), 4646-4655. DOI: 10.1016/j.biortech.2010.01.112
- Shimada, N., Kawamoto, H., and Saka, S. (2008). "Different action of alkali/alkaline earth metal chlorides on cellulose pyrolysis," *J. Anal. Appl. Pyrolysis* 81(1), 80-87. DOI: 10.1016/j.jaap.2007.09.005
- Soncini, R. M., Means, N. C., and Weiland, N. T. (2013). "Co-pyrolysis of low rank coals and biomass: Product distributions," *Fuel* 112, 74-82. DOI: 10.1016/j.fuel.2013.04.073
- Sonobe, T., Worasuwannarak, N., and Pipatmanomai, S. (2008). "Synergies in co-pyrolysis of Thai lignite and corncob," *Fuel Process. Technol.* 89(12), 1371-1378. DOI: 10.1016/j.fuproc.2008.06.006
- Wang, B., Zhao, S., Huang, Y., and Zhang, J. (2014). "Effect of some natural minerals on transformation behavior of sulfur during pyrolysis of coal and biomass," *J. Anal. Appl. Pyrolysis.* 105, 284-294. DOI: 10.1016/j.jaap.2013.11.015
- Wei, L., Zhang, L., and Xu, S. (2011). "Effects of feedstock on co-pyrolysis of biomass and coal in a free-fall reactor," *J. Fuel Chem. Technol.* 39(10), 728-734. DOI: 10.1016/s1872-5813(11)60044-3
- Weiland, N. T., Means, N. C., and Morreale, B. D. (2012). "Product distributions from isothermal co-pyrolysis of coal and biomass," *Fuel* 94, 563-570.
- Yang, X., Yuan, C., Xu, J., and Zhang, W. (2014). "Co-pyrolysis of Chinese lignite and biomass in a vacuum reactor," *Bioresour. Technol.* 173, 1-5. DOI: 10.1016/j.biortech.2014.09.073

- Zhang, M., Resende, F., and Moutsoglou, A. (2012). "Pyrolysis of lignin extracted from prairie cordgrass, aspen, and kraft lignin by Py-GC/MS and TGA/FTIR," *J. Anal. Appl. Pyrolysis* 98, 65-71. DOI: 10.1016/j.jaap.2012.05.009
- Zhang, X., Yang, W., and Dong, C. (2013). "Levoglucosan formation mechanisms during cellulose pyrolysis," *J. Anal. Appl. Pyrolysis* 104, 19-27. DOI: 10.1016/j.jaap.2013.09.015

Article submitted: June 22, 2015; Peer review completed: September 12, 2015; Revised version received and accepted: September 20, 2015; Published: September 28, 2015.  
DOI: 10.15376/biores.10.4.7667-7680